

The Extragalactic Lens VLBI Imaging Survey (ELVIS): Searching for Central Images

Edward Boyce (JBO), Steven Myers (NRAO), Joshua Winn, Jacqueline Hewitt (MKI)

Target	S_A (mJy)	S_A/S_B	Sep.	z_L	z_S	Reference
CLASS B0445+123	17	6	1''34	0.558	-	Argo et al., MNRAS, 338, 957
CLASS B0631+519	46	9	1''16	0.620	-	York et al., MNRAS, 361, 259
CLASS B0739+366	31	6	0''54	-	-	Marlow et al., AJ, 121, 619
CLASS B0850+054	49	6	0''68	0.588	-	Biggs et al., MNRAS, 338, 1084
CLASS B1152+199	52	3	1''56	0.439	1.109	Myers et al., AJ, 117, 2565
PMN J1838-3427	145	14	1''00	0.36?	2.78	Winn et al., AJ, 120, 2868
CLASS B2319+051	40	5	1''36	0.624	-	Rusin et al., AJ, 122, 591

Table 1: the ELVIS sample. Central images are brightest in "asymmetric" lenses, those with two images at a high flux density ratio, and must be observed in the radio to avoid extinction of the images by dust in the lens galaxy. ELVIS includes all the radio-loud lenses with two images at a flux density ratio $> 5:1$ except B1030+074, which was the subject of a similar study (Zhang et al. 2007, MNRAS, accepted, /astro-ph/0703226).

Observations

□ We made sensitive VLBI observations of 7 gravitational lenses at 5 or 8.4 GHz, either 27-44 hours with the Very Long Baseline Array (VLBA), or 2-8 hours with the High Sensitivity Array (HSA; VLBA in combination with Green Bank, Arecibo, phased VLA and/or Effelsberg). In each case we did not detect a central image, but improved the upper limit on its flux density.

□ We analysed the recovery of faint sources at these high dynamic ranges, finding that the process is not straightforward. We introduced faint artificial point sources in the region where the central image might be found, and measured the flux density at these locations in the final map. We had to impose a limit of 1 or 2 cycles of self-calibration, where each cycle consisted of mapping, phase self-calibration on the bright lensed images, mapping, and then phase and amplitude self-calibration on the bright lensed images. Further self-calibration made slight improvements to the blank field rms, but reduced the flux density of a faint artificial source drastically. B0631+519 and B0850+054 had relatively poor u-v coverage (due to the lack of Arecibo and Green Bank, respectively), which led to very poor recovery of faint sources for these targets even with minimal self-calibration.

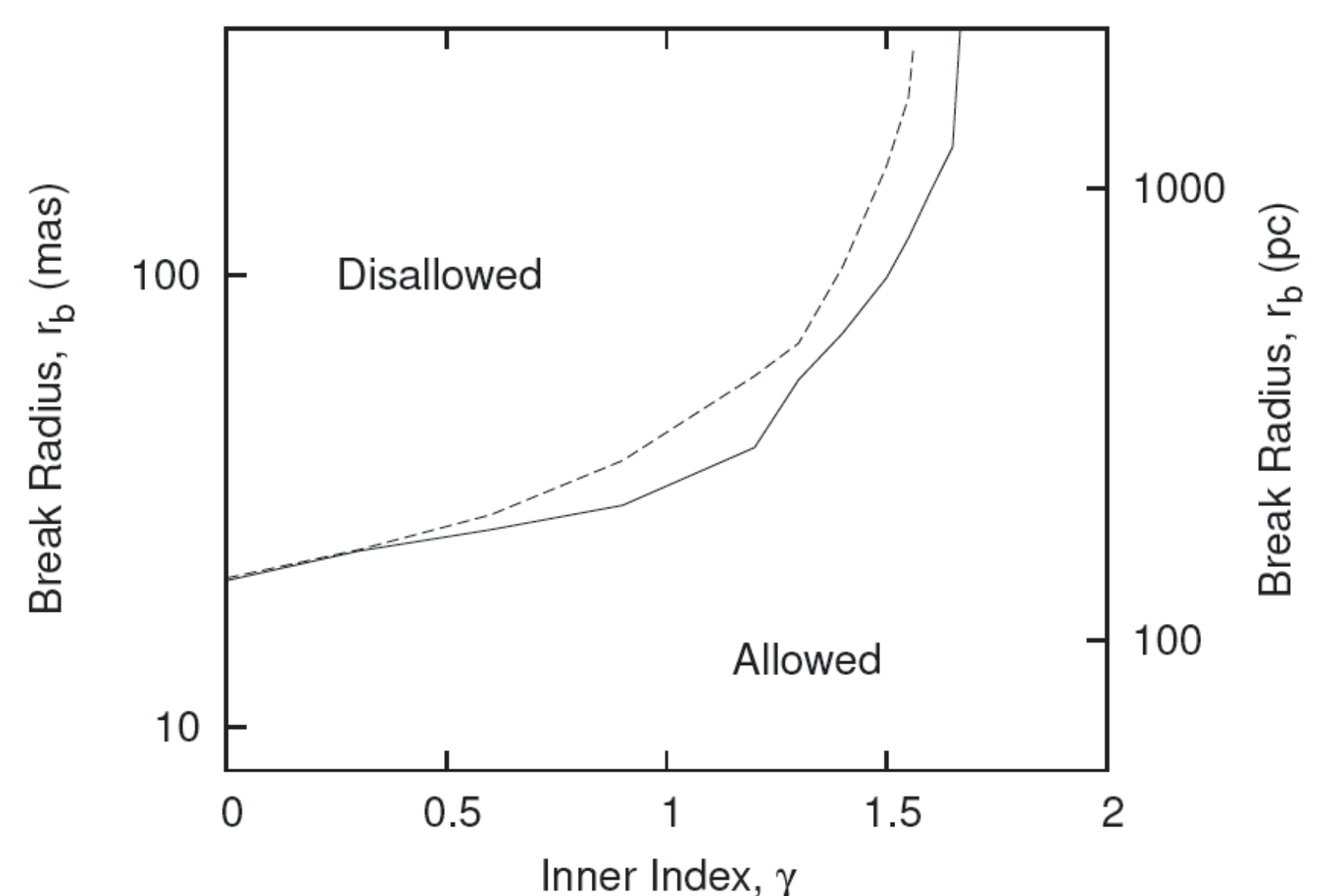


Figure 2: Mass model constraints on B0445+123. The lines show the allowed region for a mass model with no black hole (bottom) and a $2 \times 10^8 M_\odot$ black hole (top). The allowed region is the 95% confidence range in break radius for each inner index, based on a Markov Chain Monte Carlo simulation.

Modelling

- The central image is a sensitive probe of the density profile in the inner few hundred pc of the lens galaxy. A steeper central profile demagnifies the central image; a profile which is isothermal or steeper eliminates it entirely. □
- Other lensing and dynamics studies indicate that early-type galaxies are well fit by an isothermal profile at radii of a few kpc (e.g. Koopmans et al. 2006, ApJ, 649, 599). We constrain a double power law density profile for the lens galaxy:

$$\rho = \frac{\rho_0}{r^\gamma} \frac{1}{(1+r^2/r_b^2)^{(n-\gamma)/2}}$$

setting the outer index $n=2$ (isothermal) and allowing the break radius r_b and the inner index γ to vary. The galaxy core / cusp must be sufficiently steep (small r_b or large γ) to make the central image too faint to be detected. Additional steepness from a central black hole allows the bulk profile to be somewhat shallower and relaxes the constraints (the black hole mass can be estimated from the isothermal model velocity dispersion using the M- σ relation).

- The constraint on γ is one-sided: the central profile can be made arbitrarily steep and it still fits the data by eliminating the central image. We use a Markov Chain Monte Carlo (MCMC) simulation, holding the inner index fixed and varying the break radius and other parameters to find the 95% allowed region for that inner index. We stop when the inner index is steep enough to allow any break radius. A faint central image would lose flux density in the mapping process (Table 2) and might appear over a large area, roughly 10^3 resolution elements in the VLBI maps, meaning that it cannot be treated as a non-detection at a single location. The MCMC code measures the flux density at the exact location predicted by any given model, and multiplies that value by the inverse of the flux density loss to obtain the observed central image flux density for that model.

Acknowledgements

We thank Neal Jackson, Ming Zhang, Ian Browne and Richard Porcas for useful discussions. The National Radio Astronomy Observatory is a facility of the National Science Foundation, operated by Associated Universities, Inc. This work was funded by NSF grant AST 00-71181, a NRAO pre-doctoral fellowship and the European Commission's Sixth Framework Marie Curie Research Training Network Programme, Contract No. MRTN-CT-2004-505183 "ANGLES."

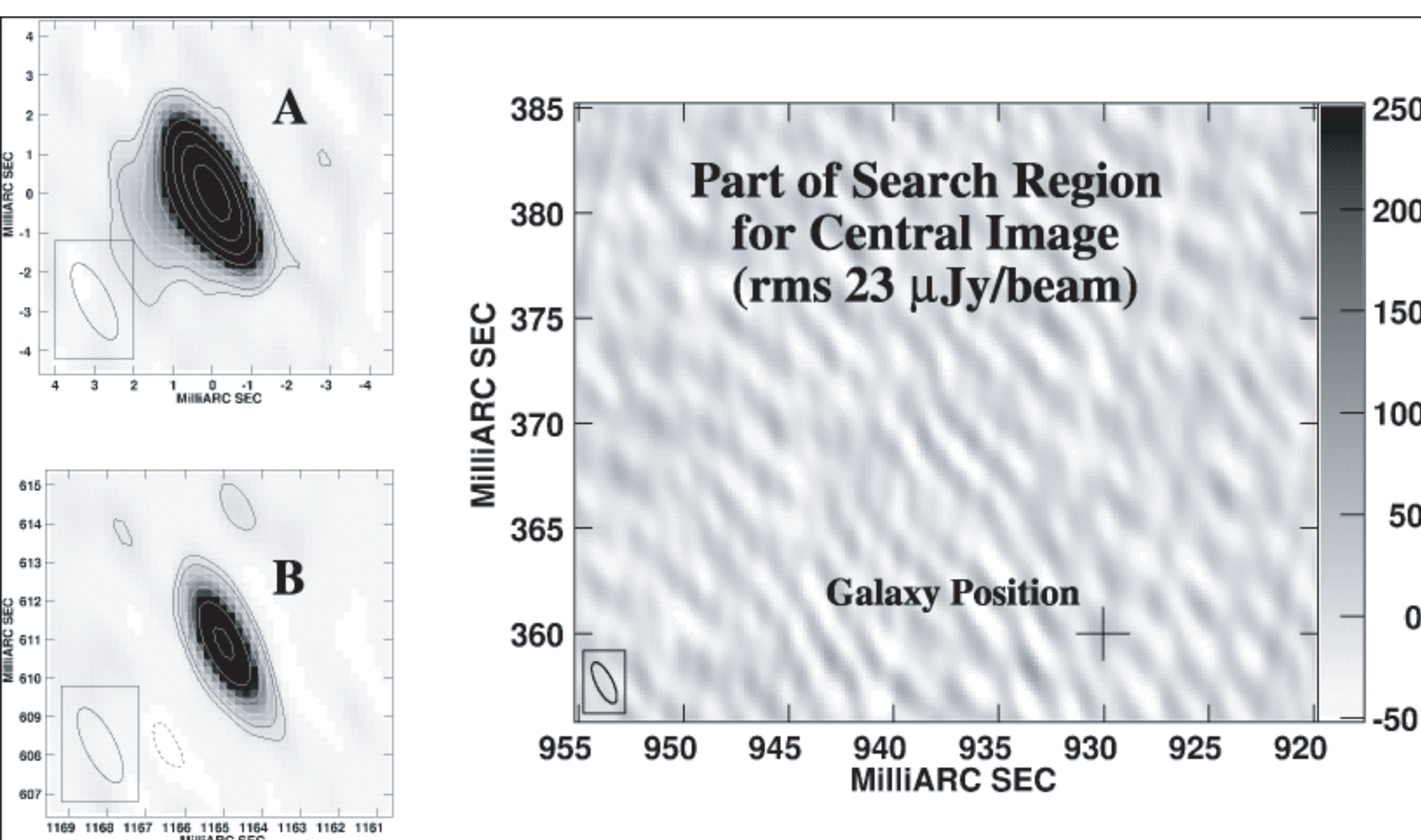


Figure 1: HSA maps of B0445+123, showing the bright images A and B (contours increase in factors of 2 from $80 \mu\text{Jy}/\text{bm}$) and the region where the central image would be found (greyscale in $\mu\text{Jy}/\text{bm}$, lens galaxy position marked by a cross).

Target	Blank Field rms ($\mu\text{Jy}/\text{bm}$)	Flux Density Loss
CLASS B0445+123	23	7%
CLASS B0631+519	20	64%
CLASS B0739+366	20	19%
CLASS B0850+054	39	66%
CLASS B1152+199	40	23%
PMN J1838-3427	43	18%
CLASS B2319+051	14	36%

Table 2: Table of observations, giving the noise in the region where a central image might appear, and the flux density lost by a faint artificial source in the imaging process. J1838-3427 and B0739+366 were observed with the VLBA, all other sources were observed with the HSA.